

1           **Variability in terrigenous sediment supply offshore of the Rio de la Plata (Uruguay)**  
2           **recording the continental climatic history over the past 1200 years**

3  
4                           L. Perez<sup>1,4\*</sup>, F. García-Rodríguez<sup>1,4</sup>, T. J. J. Hanebuth<sup>2,3</sup>

5   <sup>1</sup> Sección Oceanología, Facultad de Ciencias, Universidad de la República, Iguá 4225, Montevideo  
6   11400 (Uruguay).

7   <sup>2</sup> School of Coastal and Marine Systems Sciences, Coastal Carolina University, SC 29528 (USA).

8   <sup>3</sup> MARUM – Center for Marine Environmental Sciences, University of Bremen, Leobener Straße,  
9   28359 Bremen (Germany).

10   <sup>4</sup> Centro Universitario Regional Este, CURE-Rocha, Ruta 9 intersección Ruta 15, Rocha  
11   (Uruguay).

12   Correspondence to: L. Perez ([lp3\\_3@hotmail.com](mailto:lp3_3@hotmail.com))

13

14

15 **Abstract**

16 The continental shelf adjacent to the Río de la Plata (RdIP) exhibits extremely complex  
17 hydrographic and ecological characteristics which are of great socio-economic importance. Since  
18 the long-term environmental variations related to the atmospheric (wind fields), hydrologic  
19 (freshwater plume), and oceanographic (currents and fronts) regimes are little known, the aim of  
20 this study is to reconstruct the changes in the terrigenous input into the inner continental shelf  
21 during the Late Holocene period (associated with the RdIP sediment discharge) and to unravel the  
22 climatic forcing mechanisms behind them. To achieve this, we retrieved a 10-m long sediment  
23 core from the RdIP mud depocenter at 57 m water depth (GeoB 13813-4). The radiocarbon age  
24 control indicated an extremely high sedimentation rate of 0,8 cm per year, encompassing the past  
25 1200 years (750-2000 AD). We used element ratios (Ti/Ca, Fe/Ca, Ti/Al, Fe/K) as regional proxies  
26 for the fluvial input signal, and the variations in relative abundance of salinity-indicative diatom  
27 groups (freshwater versus marine-brackish), to assess the variability in terrigenous freshwater and  
28 sediment discharges. Ti/Ca, Fe/Ca, Ti/Al, Fe/K and the freshwater diatom group showed the lowest  
29 values between 850 and 1300 AD, while the highest values occurred between 1300 and 1850 AD.

30 The variations in the sedimentary record can be attributed to the Medieval Climatic Anomaly  
31 (MCA) and the Little Ice Age (LIA), both of which had a significant impact on rainfall and wind  
32 patterns over the region. During the MCA, a weakening of the South American Summer Monsoon  
33 System (SAMS) and the South Atlantic Convergence Zone (SACZ), could explain the lowest  
34 element ratios (indicative of a lower terrigenous input) and a marine-dominated diatom record,  
35 both indicative of a reduced RdIP freshwater plume. In contrast during the LIA, a strengthening of  
36 SAMS and SACZ, may have led to an expansion of the RdIP river plume to the far north, as  
37 indicated by higher element ratios and a marked freshwater diatom signal. Furthermore, a possible  
38 multi-decadal oscillation probably associated with Atlantic Multidecadal Oscillation (AMO) since  
39 1300 AD, reflects the variability in both the SAMS and SACZ systems.

40 **Keywords**

41 Terrigenous sediment supply, element ratios, salinity-indicative diatom groups, historical climatic  
42 changes, South American Summer Monsoon System, South Atlantic Convergence Zone, Río de  
43 la Plata, mud depocenter, continental shelf, Uruguay.

## 44 **1 Introduction**

45 The Río de la Plata (RdIP) estuary is fed by the Paraná and the Uruguay Rivers and drains into the  
46 Southwestern Atlantic Ocean (SWAO) forming the second largest estuary system in South  
47 America (Bisbal, 1995; Acha et al., 2003). The RdIP is the main source of continental freshwater  
48 and sediments entering the SWAO (Piola et al., 2008; Krastel et al., 2011, 2012; Razik et al., 2013;  
49 Lantzsich et al., 2014; Nagai et al., 2014). In this sense, the RdIP provides an average annual  
50 suspended sediment load of  $79.8 \times 10^6$  tons  $\text{yr}^{-1}$  (Depetris et al., 2003). Most of this discharge is  
51 directed close to the Uruguayan coast towards the inner continental shelf (Depetris et al., 2003;  
52 Gilberto et al., 2004). The RdIP freshwater discharge, leads to a low salinity plume on the inner  
53 continental shelf, which can reach northerly areas up to  $28^\circ\text{S}$  (Piola et al., 2000). The low-salinity  
54 waters on the inner part of the continental shelf extend downwards to a depth of approximately 50  
55 m, while the outer part of the continental shelf (from 50 m to 200 m) is influenced by the  
56 Subtropical Confluence, where the warm, salty southward-flowing Brazil Current collides with the  
57 cold and less salty northward-flowing Malvinas Current (Piola et al., 2000).

58 The Paraná River contributes about 73% to the total RdIP freshwater discharge and maximum  
59 values are found during austral summer (Depetris and Pasquini, 2007). This precipitation and river  
60 discharge pattern is associated with the southward expansion and intensification of the South  
61 American Summer Monsoon System (SAMS; Zhou and Lau, 1998; Chiessi et al., 2009). The  
62 SAMS is known to be a poleward displacement of the Intertropical Convergence Zone (ITCZ),  
63 and it is associated with a wet season that begins in the equatorial Amazon and propagates rapidly  
64 eastward and southeastward during austral spring (García and Kayano, 2010). The SAMS is tightly  
65 associated with the South Atlantic Convergence Zone (SACZ, Carvalho et al., 2004), which is a  
66 main component of the SAMS (Nogués-Paegle et al., 2002; Almeida et al., 2007). The SACZ is  
67 an elongated NW-SE band of convective activity that originates in the Amazon Basin, which  
68 extends above the northern RdIP drainage basin, and has its southernmost limit in the adjacent  
69 SWAO (Carvalho et al., 2004). Thus, the Paraná River discharge is largely determined by the  
70 SACZ (Robertson and Mechoso, 2000).

71 The RdIP is an extremely dynamic system which exhibits complex hydrodynamic features  
72 associated with the climatic pattern that affect the wind and oceanographic systems, as well as the

73 river discharge (Piola et al., 2008). As mentioned above, a natural intra-annual variability exists  
74 with a higher river discharge during the summer season (Depetris and Pasquini, 2007). Besides, a  
75 northerly wind pattern during summer leads to a southward and offshore displacement of the low-  
76 salinity RdIP freshwater plume (Guerrero et al., 1997; Möller et al., 2008; Piola et al., 2008). In  
77 contrast during the winter season, existed a lower RdIP discharge, but exists a predominant  
78 southerly wind pattern (associated with a northward displacement of the Westerlies). This situation  
79 forces a northward displacement of the RdIP plume and thus, considerably diminishes the salinity  
80 on the southern Brazilian continental shelf (Guerrero et al., 1997; Camilloni, 2005; Möller et al.,  
81 2008; Piola et al., 2008).

82 The regional climatic system also exhibits an inter-annual and inter-decadal variability, associated  
83 with environmental changes (expressed mainly in precipitation patterns) related to the El Niño/La  
84 Niña Southern Oscillation (ENSO) and the Pacific Decadal Oscillation (PDO), respectively  
85 (Depetris and Kempe, 1990; Depetris et al., 2003; Depetris and Pasquini, 2007; Garreaud et al.,  
86 2009; Barreiro, 2010). PDO is associated with ENSO as both seem to produce similar climatic  
87 effects, though their mechanisms are not yet fully understood (Garreaud et al., 2009). In this sense,  
88 it has been suggested that during both the warm El Niño and the positive PDO phases, there is an  
89 increasing trend in precipitations over the RdIP drainage basin associated with an intensification  
90 of the SAMS, which leads to a higher RdIP river discharge, while the opposite trend was observed  
91 for the negative phases (Ciotti et al., 1995; Depetris and Pasquini, 2007; Garreaud et al., 2009;  
92 Barreiro, 2010; García-Rodríguez et al., 2014). However, Piola et al (2005) reported strong NE  
93 winds during El Niño conditions which compensate the effect of the positive precipitation  
94 anomalies, and thus prevent an anomalous northeastward displacement of the RdIP plume. In  
95 addition, there is evidence that the interannual variability in the RdIP drainage basin has a stronger  
96 influence on the Uruguay River discharge, whilst the decadal variability is most pronounced in the  
97 Paraná River supply (Robertson and Mechoso, 2000). Furthermore, Chiessi et al. (2009) published  
98 evidence that the Atlantic Multidecadal Oscillation (AMO) influences SAMS intensity on the  
99 multidecadal time scales, leading to reduced/increased SAMS intensity when the AMO is in its  
100 positive/negative phase (Chiessi et al., 2009; Apaéstegui et al., 2014).

101 Regarding the Late Holocene period, a significant number of studies has described the climatic  
102 history of South America over the last 1500 cal yr BP (calibrated thousands of years before

103 present), i.e., for the Medieval Climatic Anomaly (MCA, 800-1300 AD) and the Little Ice Age  
104 (LIA, 1400-1800 AD), (Cioccale, 1999; Iriondo, 1999; Piovano et al., 2009; Bird et al., 2011b; del  
105 Puerto et al., 2011; Vuille et al., 2012; del Puerto et al., 2013; Apaéstegui et al., 2014; Salvatecci  
106 et al., 2014). These climatic changes have affected the precipitation pattern over South America  
107 with regional differences. For eastern Uruguay, this means a warmer and more humid pulse during  
108 the MCA, while in the LIA, a drier and colder climate was recorded (del Puerto et al., 2013).  
109 Piovano et al. (2009) have inferred similar climatic conditions for the northeastern region of  
110 Argentina. In contrast, the opposite pattern was reported for southern Chile and Argentina, where  
111 a dry period occurred during the MCA, and a wetter pulse governed the LIA (Haberzettl et al.,  
112 2005). Furthermore, Vuille et al. (2012) reported similar conditions for southeastern Brazil as  
113 Haberzettl et al. (2005).

114 Nevertheless, little is known about how the natural climatic variability over South America affects  
115 sedimentation, salinity and river discharge on the continental shelf in front of the RdIP, during the  
116 Late Holocene period (Burone et al., 2012; Perez et al., in press). The aim of this study therefore,  
117 is to determine the variations in the terrigenous sediment input into the ocean over the last 1200  
118 cal yr BP. To determine how the continental influence competed with the marine regime, a 10-m  
119 long sediment core was taken from a confined mud depocenter on the inner Uruguayan continental  
120 shelf (GeoB 13813-4, Fig. 1). The sedimentary succession of this core was analyzed for major  
121 chemical elements (Ca, Ti, Al, Fe, and K) and compared with previously published data of the  
122 diatom salinity-indicative groups, i.e. freshwater (F) and marine, marine-brackish (M-B), (Perez  
123 et al. in press) in order to assess variations in continental influence.

## 124 **2 Study Area**

125 The study area is located on the Uruguayan inner continental shelf hosting the RdIP mud  
126 depocenter (50 m water depth, Fig. 1a, b). This silty clay depocenter (Martins and Urien, 2004;  
127 Lantzsich et al., 2014) is the result of regional paleogeographic evolution and is associated with  
128 deposits of fluvial origin (Urien and Ewing, 1974). The depocenter built up inside the RdIP paleo-  
129 valley which was incised by the Paleo-Paraná River during lower sea levels (Masello and Menafrá,  
130 1998; Martins et al., 2003; Lantzsich et al., 2014; Hanebuth et al., in press). The RdIP paleo-valley  
131 depression offers an effective protection against the generally strong hydrodynamic conditions on

132 the shelf, thus favoring the deposition and preservation of these muds (Fig. 1b).

### 133 **3 Materials and Methods**

134 A 1028-cm long sediment core (GeoB 13813-4) was taken from the RdIP mud depocenter  
135 (34°44'13" S, 53°33'16" W) during research cruise M76/3a with the German research vessel  
136 "Meteor" in July 2009 (Krastel et al., 2012; Fig. 1a). During this expedition, sub-bottom profiling  
137 with the shipboard PARASOUND system (4 kHz) showed an elongated depression on the seafloor  
138 corresponding to the RdIP paleo-valley filled with a complex pattern of acoustic facies (Fig. 1b,  
139 Krastel et al., 2012; Lantzsich et al., 2014).

#### 140 **3.1 Age-depth model and sedimentation rates**

141 Material from bivalve shells collected from six sediment samples, distributed evenly over the core  
142 and preserved in life position, were used for radiocarbon dating ( $^{14}\text{C}$ ), (Table 1, Lantzsich et al.,  
143 2014; Perez et al., in press). The samples were analyzed using AMS- $^{14}\text{C}$  (accelerated mass  
144 spectrometry) at the Poznan Radiocarbon Laboratory in Poland. The age depth model used for this  
145 study was then generated by using the free software Bacon (Blaauw and Christen, 2011, Fig. 2).  
146 The raw  $^{14}\text{C}$  dates were calibrated using the calibration curve Marine13 (Reimer et al., 2013, cc=2)  
147 integrated into this program, and the weighted average ages are expressed in table 1 (Blaauw and  
148 Christen, 2011). The standard reservoir age of 405 years was applied during calibration due to a  
149 lack of regional data, although intense water mixing and coastal upwelling in shallow waters might  
150 lead to significant differences in reservoir age (Reimer et al. 2013).

151 Bacon software is an approach for developing an age-depth model that uses Bayesian statistics to  
152 reconstruct Bayesian accumulation histories for sedimentary deposits. Bacon divides a sediment  
153 core into vertical sections (5 cm thick), and estimates the sedimentation rate (years/cm) for each  
154 section through millions of Markov Chain Monte Carlo (MCMC) iterations.

#### 155 **3.2 Paleo-environmental proxies**

156 The two methodological approaches combined in this study were chosen according to previous  
157 successful applications for inferring continental versus marine influences in the Atlantic Ocean,  
158 (Romero et al., 1999; Chiessi et al., 2009; Mahiques et al., 2009; Govin et al., 2012; Burone et al.,

159 2013; Perez et al., in press), as indicated below.

### 160 **3.2.1 Runoff-indicative element ratios**

161 The relative concentrations (expressed in counts per second, cps) of the major chemical elements  
162 used in this study (Ca, Ti, Fe, K, Al) were obtained by an X-ray fluorescent (XRF) sediment core  
163 scanner AVAATECH at MARUM, University of Bremen. XRF core scanning is a fast, non-  
164 destructive technique, which allows for the detection of a large number of chemical elements  
165 (Löwemark et al., 2011). This technique does not measure absolute element concentrations, but  
166 relative intensities. As a consequence, the intensities of the elements are influenced by numerous  
167 factors such as water content and sediment density, organic matter content, grain size, biogenic  
168 contributions, and carbonate dissolution (Weltje and Tjallingii, 2008). For these reasons, it is  
169 unwise to use single element intensities, and it is more appropriate to use element ratios to  
170 normalize the data (Weltje and Tjallingii, 2008; Francus et al., 2009; Govin et al., 2012). Core  
171 GeoB 13813-4 was scanned in 1-cm steps throughout, and the Ti/Ca, Fe/Ca, Fe/K and Ti/Al  
172 element ratios were used.

173 Ti, Fe and Al are elements related to aluminum/silicates, and are associated with clay minerals  
174 carried from the continent as weathering products, and through river discharge, they enter into the  
175 ocean (Goldberg and Arrhenius, 1958; Jansen et al., 1992; Yarincik et al., 2000). Therefore these  
176 elements vary with the terrigenous portion in offshore sediment (Martins et al., 2007; Burone et  
177 al., 2013). Most of the K in marine sediments is also associated with terrigenous materials  
178 (Goldberg and Arrhenius, 1958), and occurs mainly in fully arid regions where chemical  
179 weathering rates are lower (Govin et al., 2009). In contrast, Ca mainly reflects the marine carbonate  
180 content in the sediment, and is thus associated with the local marine productivity (Haug et al.,  
181 2001; Salazar et al., 2004; Gonzalez-Mora and Sierro, 2007). Al, Ti and K are little affected by  
182 biological and redox variations, whilst Fe is sometimes altered by redox processes (Jansen et al.,  
183 1992; Yarincik et al., 2000; Löwemark et al., 2011). Burone et al. (2013) recorded a decreasing  
184 seaward gradient in Ti, Fe, Al from surface sediment transect from the inner RdIP off to the shelf.  
185 In addition, they observed the opposite trend for Ca.

186 Numerous studies used major elements in marine sediments to reconstruct climatic history, but the

187 choice of particular element ratios and the interpretation of such proxies vary from site to site  
188 (Govin et al., 2012). Ti/Ca and Fe/Ca ratios were widely used to reconstruct the continental versus  
189 the marine influence in the SWAO region (Chiessi et al., 2009; Mahiques et al., 2009; Govin et  
190 al., 2012; Bender et al., 2013; Burone et al., 2013). On the other hand, Fe/K and Ti/Al ratio was  
191 used in South America to reflect the degree of chemical weathering in areas without significant  
192 eolian input (Govin et al., 2012), such as the case of the RdIP (Mahowald et al., 2006). As a  
193 consequence of the mentioned above, we used element ratios (Ti/Ca, Fe/Ca, Ti/Al, Fe/K) as  
194 regional proxies for the fluvial input signal on the inner Uruguayan continental shelf.

### 195 **3.2.2 Salinity-indicative diatom groups**

196 Samples for diatom analyses were first chemically treated (with the aim of cleaning the material  
197 from carbonates, organic matter and clay particles) as explain in Perez et al. (in press). Diatom  
198 samples were first treated with Na<sub>2</sub>P<sub>2</sub>O<sub>7</sub> to deflocculate the sediment and eliminate clay particles.  
199 The samples were then treated with a 35 % HCl to remove inorganic carbonate material. Finally,  
200 the samples were boiled in 30 % H<sub>2</sub>O<sub>2</sub> for two hours to eliminate organic matter (Metzeltin and  
201 García-Rodríguez, 2003). Between each treatment, samples were rinsed at least four times with  
202 distilled water. Permanent sediment slides were mounted using the Entellan® mounting medium.  
203 A minimum of 400 valves was counted on each slide with a light microscope at 1250 x  
204 magnification. The diatoms were then identified and counted at 10 cm depth intervals throughout  
205 the sediment core and in 1 cm steps within the uppermost 100 cm (Perez et al., in press). Diatom  
206 species were identified and separated into two groups according to their ecological salinity  
207 preference, i.e., in groups indicating freshwater (F) and marine/marine-brackish (M-B) conditions,  
208 according to Frenguelli (1941, 1945), Müller-Melchers (1945, 1953, 1959), Hasle and Syversten  
209 (1996), Witkowski et al. (2000), Metzeltin and García-Rodríguez (2003), Metzeltin et al. (2005),  
210 Hassan et al. 2010, Sar et al. (2010) and other standard diatom literature (Perez et al., in press).

211 Romero et al. (1999) determined variations in the continental water discharge by using freshwater  
212 diatoms (especially from the genus *Aulacoseira*) along a sediment surface transect from the eastern  
213 South Atlantic coast to the open ocean. The same approach was also used in this study to evaluate  
214 the freshwater influx on the inner continental shelf.



## 215 **4 Results**

### 216 **4.1 Age-depth model and sedimentation rates**

217 The core's base was dated to 1200 cal yr BP (750 AD), while a sample at 255 cm was dated to 230  
218 cal yr BP (1700 AD, Table 1). The sedimentation rate varied between 0.68 and 1.0 cm yr<sup>-1</sup>, with a  
219 mean sedimentation rate of 0.8 cm yr<sup>-1</sup>. Minimum values were observed in the top section (i.e., at  
220 200 to 350 cm) and in the bottom section (i.e., at 705 to 967 cm), while the highest values were  
221 observed in the middle of the core (at 500 to 705 cm, Perez et al., in press).

### 222 **4.2 Paleo-environmental proxies**

#### 223 **4.2.1 Runoff-indicative element ratios**

224 All the element ratios (Ti/Al, Fe/K, Ti/Ca and Fe/Ca) showed similar profiles (Fig. 3). The lowest  
225 values were recorded between 850-1300 AD (coinciding with the MCA), and remained stable  
226 during this interval of time. In contrast, high values were recorded from 1300 to 1850 AD  
227 (associated with the LIA) and showed a high variability with a number of sharp maxima. In that  
228 sense, for the Ti/Al and Fe/K ratios we recorded, a succession of peaks and lows approximately  
229 every 100 years (from 1300 to 1500 AD) and every 50 years (1500 AD up to the present), (Fig. 3).  
230 Moreover during the last century, all element ratios showed a rapid increase toward the highest  
231 measured values, most pronounced over the last 50 years (Fig. 3).

#### 232 **4.2.2 Salinity-indicative diatom groups**

233 Regarding the salinity-indicative diatom groups as shown in Perez et al. (in press), the profile of  
234 Group F seems to generally run parallel to those of the four element ratios with lower percentages  
235 around 20 % during the MCA times, and higher up to 60 %, rising and more variable values during  
236 the LIA period (Fig. 3). An exception is observed for the last 50 yr BP where the percentages  
237 declined rapidly towards the former values counted for the MCA time interval. In contrast, the  
238 Group M-B ranged from 30 to 80 % generally describing the expected opposite trend compared to  
239 the F group (Fig. 3). Over the last 100 yr BP (1900 AD up to the present), an increasing rapid trend  
240 coincides with the highest values shown for the element ratios (Fig. 3).

## 241 **5 Interpretation and Discussion**

### 242 **5.1 Age-depth model and sedimentation rates**

243 The RdIP mud depocenter shows an exceptionally high sedimentation rate ( $0.8 \text{ cm yr}^{-1}$  on average,  
244 Perez et al., in press) compared with other records from the southern Brazilian continental shelf  
245 (Mahiques et al., 2009; Chiessi et al., 2014). This high sedimentation rate is consequence of the  
246 enormous amount of sediment transported by the Paraná and Uruguay Rivers into the RdIP  
247 watershed and further onto the Uruguayan shelf (Lantzsch et al., 2014). In addition, an  
248 amplification of the sedimentation rate could be a consequence of the fact that the RdIP paleo-  
249 valley depression offers protection against strong hydrodynamic conditions on the shelf, favoring  
250 the deposition of sediments (Lantzsch et al., 2014; Hanebuth et al., in press). The beginning of  
251 sedimentation is possibly associated with the establishment of humidity conditions in the Late  
252 Holocene which have resulted in an increasing RdIP River discharge, as well as a significant  
253 sedimentation of terrigenous material over the RdIP paleo-valley (Urien et al., 1980; Iriondo, 1999;  
254 Mahiques et al., 2009; Lantzsch et al., 2014; Perez et al., in press).

### 255 **5.2 Paleo-environmental proxy records**

256 The proxy data used in this study are correlated positively with each other (excluding the last  
257 century), and reveal the direct influence of the RdIP as a source of terrigenous sediments within  
258 the inner Uruguayan continental shelf.

259 The element ratios Ti/Ca and Fe/ Ca indicates, as do other geochemical and biological proxies, a  
260 mixed fluvio-marine signal on the inner Uruguayan continental shelf, spanning over the last 1200  
261 years (Perez et al., in press). Ti and Fe are supplied from the RdIP watershed (Depetris et al., 2003),  
262 whilst Ca is an element associated with calcareous organisms such as small mollusks, forams and  
263 coccolithophorides in the ocean, and therefore it is related to the marine-biogenic productivity of  
264 the continental shelf (Depetris and Pasquini, 2007; Govin et al., 2012; Razik et al., 2013). Thus  
265 the variability in these element ratios indicates different degrees of continental influence in the  
266 study area during the Late Holocene.

267 The results of the proxies integral analysis have been linked to general climatic changes that have

268 occurred on a regional to global scale (Fig.3), and allow us to infer three major time intervals, i.e.,  
269 the MCA, the LIA and the current warm period (Mann et al. 2009), all of which were characterized  
270 by changing continental versus marine influences in the study area.

271 The oldest recorded period, from 800 to 1300 AD, is closely associated with the MCA (reported  
272 as a positive temperature anomaly in the northern hemisphere, Bradley et al., 2008; Mann et al.,  
273 2009). During this period, a strong and steady influence of marine conditions governed the inner  
274 Uruguayan continental shelf (inferred by low values of Ti/Ca and Fe/Ca, and a dominance of the  
275 M-B diatom salinity group), probably as a result of a weakened RdIP water and terrigenous  
276 sediment discharge. This situation led to a major and more constant sedimentation of marine  
277 particulate carbon during the MCA (Perez et al., in press). In addition, the low Fe/K values  
278 registered during the MCA would suggest conditions of reduced RdIP river discharge and dry  
279 conditions over the drainage basin (Vuille et al., 2012). Climatically drier conditions appear to  
280 decrease chemical weathering in the Fe-rich RdIP drainage basin, thus depleting the Fe content in  
281 the offshore depocenters in relation to K, which is associated with drier conditions (Depetris et al.,  
282 2003; Depetris and Pasquini et al., 2007).

283 Our findings, combined with those reported in other studies, suggest a weakened SAMS during  
284 the MCA (Fig. 4, Bird et al., 2011a; Bird et al., 2011b; Vuille et al., 2012; Apaéstegui et al., 2014;  
285 Salvatecci et al., 2014). Though the continental SAMS exhibits spatial-temporal characteristics  
286 that differ from the ITCZ, the latitudinal position of the ITCZ is closely related to changes in the  
287 SAMS intensity, and both climatic elements also respond to temperature anomalies in the northern  
288 hemisphere, especially in the north Atlantic (Table 2, Stríkis et al., 2011; Bird et al., 2011b; Vuille  
289 et al., 2012; Apaéstegui et al., 2014). In this sense, positive/negative northern hemisphere  
290 temperature anomalies are linked to the north/south directional migration of the ITCZ thus  
291 diminishing/increasing SAMS activity (Broccoli et al., 2006; Bird et al., 2011b; Stríkis et al., 2011;  
292 Vuille et al., 2012). Hence, the positive temperature anomalies in the northern hemisphere during  
293 the MCA (Mann et al., 2009; probably associated with a positive phase of the AMO), led to  
294 reduced SAMS and SACZ intensity, in addition to a northward displacement of the ITCZ (Fig. 4,  
295 Chiessi et al., 2009; Bird et al., 2011b; Stríkis et al., 2011; Vuille et al., 2012; Apaéstegui et al.,  
296 2014). Such atmospheric conditions during the MCA led to a significant decrease in rainfall over  
297 the RdIP watershed (mainly in the catchment area of its main tributary, the Paraná River; Robertson

298 and Mechoso, 2000). As a consequence of this, we inferred a reduction in both freshwater and  
299 sediment input, in conjunction with an increase in salinity (Perez et al., in press) on the Uruguayan  
300 continental shelf. The decrease in SACZ activity during the MCA could also help explain the more  
301 humid conditions inferred for Uruguay during this episode (del Puerto et al., 2013). This is  
302 associated with an increase in precipitation over the Uruguay River drainage basins due to a  
303 reduced SACZ intensity as discuss below (Robertson and Mechoso, 2000).

304 The following period, from 1300 to 1850 AD, coincided with the LIA as reported for the northern  
305 hemisphere (Bradley et al., 2003; Mann et al., 2009). This period is characterized by higher values  
306 of Ti/Al, Fe/K, Ti/Ca and Fe/Ca than those recorded during the preceding period (Fig. 3).  
307 Therefore, we recorded a higher content of terrigenous material rich in Ti and Fe from the RdIP  
308 watershed (Depetris et al., 2003; Depetris and Pasquini, 2007) which is associated with a higher  
309 river discharge during the LIA. Furthermore, a dominance of F diatoms was detected (Fig. 3). The  
310 F diatom group was mainly dominated by *Aulacoseira* spp., especially *A. granulata* (Perez et al.,  
311 in press), which is the most common diatom genus from the Paraná River and the inner RdIP  
312 (Gomez and Bauer, 2002; Licursi et al., 2006; Devercelli et al., 2014). Moreover, Massaferrero et  
313 al. (2014) observed that the F diatom group recorded in the uppermost 55 cm of the sediment core  
314 GeoB 13813-4 was associated with the positive anomalies of the Paraná River discharges. Thus,  
315 all the proxies indicate wetter conditions over the RdIP drainage basin, and consequently, a major  
316 freshwater supply from the RdIP to the inner Uruguayan shelf during the LIA. Accordingly, we  
317 observed the highest rates of terrigenous deposition during this episode.

318 The LIA, characterized by cold conditions over the northern hemisphere, was then related to a  
319 strengthening of SAMS and SACZ (Fig. 4, Bird et al., 2011b; Vuille et al., 2012; Apaéstegui et  
320 al., 2014). This leads to both a reduction in rainfall rates over northern South America, Central  
321 America and Mexico (Haug et al., 2001; Vazques-Castro et al., 2008), and elevated rainfall rates  
322 in the Andes (Sifeddine et al., 2008; Bird et al., 2011a; Bird et al., 2011b; Vuille et al., 2012;  
323 Apaéstegui et al., 2014; Salvatecci et al., 2014), and over SESA (Meyer and Wagner, 2009; Vuille  
324 et al., 2012). The intensification and northward displacement of the Southern Westerlies during  
325 the LIA was also registered (Moy et al., 2009; Koffman et al., 2014). This, in conjunction with a  
326 higher river discharge, would have also caused an anomalous northward shift of the RdIP river  
327 plume. Such atmospheric conditions during the LIA have led to a significant increase in rainfall

328 over the RdIP watershed. Therefore, the outcome was a higher influence of the RdIP river plume  
329 within the inner Uruguayan continental shelf as recorded in this study.

330 The succession of maximum and minimum peaks in the element ratios from 1300 AD to present  
331 (every 50 to 100 years), suggests an influence of the AMO on RdIP river discharge related to  
332 changes in SAMS and SACZ intensity (Chiessi et al., 2009; Stríkis et al., 2011). The AMO  
333 significantly affects the SAMS at multi-decadal time scales, leading to a reduced SAMS intensity  
334 when the AMO is in its positive phase, and the ITCZ retreats northward, leading to a decrease in  
335 RdIP river discharge (Table 2, Chiessi et al., 2009; Strikis et al., 2011; Bird et al., 2011b;  
336 Apaéstequi et al., 2014).

337 An increase in SACZ intensity during the LIA and its decrease during the MCA, inferred in this  
338 study, explain the contrasting spatial/temporal climatic conditions recorded in the two regions in  
339 the RdIP drainage basin (SE Brazil: Vuille et al., 2012; Uruguay: del Puerto et al., 2013). SACZ  
340 intensity is associated with increased river runoff in the northern region of the RdIP catchment  
341 area (Paraná River) and a decreased runoff in the southern area (Uruguay River; Robertson and  
342 Mechoso, 2000). The north/south river runoff contrast, in response to an intensified/weakened  
343 SACZ appear to transport less/more moisture over the Uruguay River basin, thus leading to an  
344 increase/decrease in precipitation during MCA/LIA over Uruguay (del Puerto et al., 2013).

## 345 **6 Conclusions**

346 The observed changes in the presented proxy records indicate variations in both the continental  
347 runoff and the marine influence, related to regional climatic variability. Therefore, we put forward  
348 the suggestion that global atmospheric changes (related to changes in SAMS and SACZ intensity)  
349 have made an impact on the hydrodynamics and consequently, on the local sedimentation regime,  
350 on the inner Uruguayan continental shelf over the past 1200 cal yr BP (750-2000 AD).

351 During the MCA (800-1300 AD) a reduction in SAMS and SACZ activities would have caused a  
352 decrease in the rainfall rate over the RdIP drainage basin, resulting in more estuarine-marine  
353 conditions predominating over a freshwater plume signal. During the LIA (1400-1800 AD) in  
354 contrast, a strengthening in SAMS and SACZ activities led to an increased precipitation over the  
355 RdIP drainage basin, reflected by stronger terrigenous influences in terms of freshwater supply on

356 the inner Uruguayan shelf. Furthermore, a possible multi-decadal oscillation probably associated  
357 with AMO since 1300 AD, reflects the variability in both the SAMS and SACZ systems.

## 358 **7 Acknowledgements**

359 We would like to express special thanks to Ines Sunesen, Eugenia Sar, M. Michel Mahiques and  
360 Carina Lange for their fruitful discussions. We would also like to thank Vivienne Pettman for her  
361 very valuable suggestions for improving the English and also Thorsten Kiefer and three  
362 anonymous reviewers for their critical comments and suggestions which undoubtedly improved  
363 the manuscript content. We acknowledge PEDECIBA (Programa para el Desarrollo de las  
364 Ciencias Básicas) Geociencias, ANII (Agencia Nacional de Investigación e Innovación), DAAD  
365 (German Academic Exchange Service), and RLB (Red Latinoamericana de Botanica) for their  
366 financial support. The authors would also like to thank to PAGES for their partially financial  
367 support of this publication. This article is an outcome of the MARUM SD2 projectas part of the  
368 DFG 543 Research Center/Excellence Cluster “The Ocean in the Earth System” at the University  
369 of Bremen.

## 370 **8 References**

371 Acha, E., Mianzan, H., Iribarne, O., Gagliardini, D., Lasta, C., and Daleo, P.: The role of  
372 the Río de la Plata bottom salinity front in accumulating debris, *Mar. Poll. Bull.*, 46, 197-202,  
373 2003.

374 Almeida, R. A. F., Nobre, P., Haarsma, R. J., and Campos, E. J. D.: Negative ocean-  
375 atmosphere feedback in the South Atlantic Convergence Zone, *Geophys. Res. Lett.*, 34, L18809,  
376 doi:10.1029/2007GL030401, 2007.

377 Apaéstegui, J., Cruz, F. W., Sifeddine, A., Vuille, M., Espinoza, J. C., Guyot, J. L., Khodri,  
378 M., Strikis, N., Santos, R. V., Cheng, H., Edwards, L., Carvalho, E., and Santini, W.: Hydroclimate  
379 variability of the northwestern Amazon Basin near the Andean foothills of Peru related to the  
380 South American Monsoon System during the last 1600 years, *Clim. Past.*, 10, 1967–1981, 2014.

381 Barreiro, M.: Influence of ENSO and the South Atlantic Ocean on climate predictability  
382 over Southeastern South America, *Clim. Dyn.*, 35, 1493-1508, doi:10.1007/S00382-009-0666-9,  
383 2010.

384 Bender, V. B., Hanebuth, T. J. J., and Chiessi, C. M.: Holocene shifts of the subtropical  
385 shelf front off Southeastern South America controlled by high and low latitude atmospheric  
386 forcings, *Paleoceanography*, 28, 1-10, doi: 10.1002/palo.20044, 2013.

387 Bird, B. W., Abbott, M. B., Rodbell, D. T., and Vuille, M.: Holocene tropical South  
388 American hydroclimate revealed from a decadal resolved lake sediment  $\delta^{18}\text{O}$  record, *Earth*  
389 *Planet. Sc. Lett.*, 310, 192–202, 2011a.

390 Bird, B. W., Abbott, M. B., Vuille, M., Rodbell, D. T., Stansella, N. D., and Rosenmeiera,  
391 M. F.: 2,300-year-long annually resolved record of the South American summer monsoon from  
392 the Peruvian Andes, *PNAS*, 108, 8583–8588, 2011b.

393 Bisbal, G. A.: The southeast South American shelf large marine ecosystem: Evolution and  
394 components, *Mar. Policy*, 19, 1, 21-38, 1995.

395 Blaauw, M., and Christen, J. A.: Flexible paleoclimate age-depth models using an  
396 autoregressive gamma process, *Bay. Anal.*, 6, 457-474, 2011.

397 Bradley, R. S., Hughes, M. K., and Diaz, H. F.: Climate in Medieval Time, *Science*, 302,  
398 404-405, 2008.

399 Broccoli, A. J., Dahl, K. A, and Stouffer, R. J.: Response of the ITCZ to Northern  
400 Hemisphere cooling, *Geophys. Res. Lett.*, 33, L01702, doi:10.1029/2005GL024546, 2006.

401 Burone, L., Centurión, V., Cibils, L., Franco-Fraguas, P., García-Rodríguez, F., García, G.,  
402 and Pérez, L.: Sedimentología y Paleoceanografía, in: Programa oceanográfico de caracterización  
403 del margen continental uruguayo-ZEE, edited by: Burone, L., Montevideo, Uruguay, 240-295,  
404 2012.

405 Burone, L., Ortega, L., Franco-Fraguas, P., Mahiques, M., García-Rodríguez, F., Venturini,  
406 N., Marin, Y., Brugnoli, E., Nagai, R., Muniz, P., Bicego, M., Figueira, R., and Salaroli, A.: A  
407 multiproxy study between the Río de la Plata and the adjacent South-western Atlantic inner shelf  
408 to asses the sediment footprint of river vs. marine influence, *Cont. shelf Res.*, 55, 141-154, 2013.

409 Camilloni, I.: Variabilidad y tendencias hidrológicas en la cuenca del Plata, in: El cambio  
410 climático en el Río de la Plata, edited by: Barros, V., Menendez, A. and Nagy, G., CIMA, Buenos  
411 Aires, 20-31, 2005.

412 Carvalho, L. M. V., Jones, C., and Liebmann, B.: The South Atlantic Convergence Zone:  
413 Intensity, Form, Persistence, and Relationships with Intraseasonal to Interannual Activity and  
414 Extreme Rainfall, *J. Climate*, 17, 88–108, 2004.

415 Chiessi, C. M., Mulitza, S., Patzold, J., Wefer, G., and Marengo, J. A.: Possible impact of  
416 the Atlantic Multidecadal Oscillation on the South American summer monsoon. *Geophys. Res.*  
417 *Let.*, 36, L21707, doi:10.1029/2009GL039914, 2009.

418 Chiessi, C. M., Mulitza, S. G., Jeroen, S. J. B., Campos, M. C., and Gurgel, M. H. C.:  
419 Variability of the Brazil Current during the late Holocene, *Palaeogeogr. Palaeoclimatol.*, 415, 28–36, doi:  
420 10.1016/j.palaeo.2013.12.005, 2014.

421 Cioccale, M.: Climatic conditions in the central region of Argentina in the last 1000 years,  
422 *Quat. Int.*, 62, 35-47, 1999.

423 Ciotti, A. M., Odebrecht, C., Fillmann, G., and Moller, O. O.: Freshwater outflow and  
424 Subtropical Convergence influence on phytoplankton biomass on the southern Brazilian  
425 continental shelf, *Cont. Shel. Res.*, 15, 14, 1737-1756, 1995.

426 del Puerto, L., García-Rodríguez, F., Bracco, R., Castiñeira, C., Blasi, A., Inda, H.,  
427 Mazzeo, N. and Rodríguez, A.: Evolución climática holocénica para el sudeste de Uruguay,  
428 Analisis multi-proxy en testigos de lagunas costeras, in: *El Holoceno en la zona costera de*  
429 *Uruguay*, edited by: García-Rodríguez, F., Universidad de la Republica (UdelaR), 117-154, 2011.

430 del Puerto, L., Bracco, R., Inda, H., Gutierrez, O., Panario, D., and García-Rodríguez, F.:  
431 Assessing links between late Holocene climate change and paleolimnological development of Peña  
432 Lagoon using opal phytoliths, physical, and geochemical proxies, *Quat. Int.*, 287, 89-100,  
433 doi:10.1016/j.quaint.2011.11.026, 2013.

434 Depetris, P.J. and Kempe, S.: The impact of the E1 Niño 1982 event on the Paraná River,  
435 its discharge and carbon transport. *Palaeogeogr. Palaeoclimatol.*, 89, 239-244, 1990.

436 Depetris, P. J. and Pasquini, A. I.: Discharge trends and flow dynamics of southern  
437 southamerican rivers draining the southern Atlantic seabord: an overview, *J. Hidrol.*, 333, 385-  
438 399, doi: 10.1016/j.hydrol.2006.09005, 2007.

439 Depetris, P. J., Probst, J-L., Pasquini, A. I. and Gaiero, D. M.: The geochemical



440 characteristics of the Paraná River suspended sediment load: an initial assessment, *Hydrol.*  
441 *Process*, 17, 1267–1277, doi: 10.1002/hyp.1283, 2003.

442 Devercelli, M., Zalocar de Domitrovic, Y., Forastier, M. E. and Meichtry de Zaburlín N.:  
443 Phytoplankton of the Paraná River Basin, *Advanc. Limnol.*, 65, 39–65, doi: 10.1127/1612-  
444 166X/2014/0065-0033, 2014.

445 Francus, P., Lamb, H., Nakawaga, T., Marshall, M., and Brown, E.: The potential of high  
446 resolution X-ray fluorescence core scanning: Applications in paleolimnology, *PAGES news* 17, 9,  
447 93-95, 2009.

448 Frenguelli, J.: Diatomeas del Río de la Plata, *Revista Museo Nacional La Plata*, III, 213-  
449 334, 1941.

450 Frenguelli, J.: Diatomeas del Platense, *Revista Museo Nacional La Plata*, III, 77-221, 1945.

451 FREPLATA: Análisis Diagnóstico Transfronterizo del Río de la Plata y su Frente  
452 Marítimo. Documento Técnico. Proyecto “Protección Ambiental del Río de la Plata y su Frente  
453 Marítimo: Prevención y Control de la Contaminación y Restauración de Hábitats”. Proyecto  
454 PNUD/GEF/RLA/99/G31, 106, 2004.

455 Garcia, S. and Kayano, M.: Some evidence on the relationship between the South American  
456 monsoon and the Atlantic ITCZ, *Theor. Appl. Climatol.*, 99, 29–38, 2010.

457 García-Rodríguez, F., Brugnoli, E., Muniz, P., Venturini, N., Burone, L., Hutton, M.,  
458 Rodríguez, M., Pita, A., Kandravicius, N., Perez, L., and Verocai, J.: Warm-phase ENSO events  
459 modulate the continental freshwater input and the trophic state of sediments in a large South  
460 American estuary. *Mar. Freshwater Res.*, 65, 1-11, 2014.

461 Garreaud, R. D., Vuille, M., Compagnucci, R., and Marengo, J.: Present-day South  
462 American climate, *Palaeogeogr. Palaeoclimatol.*, 281, 3-4, 180-195, 2009.

463 Giberto, D. A., Bremec, C. S., Acha, E. M., and Mianzan, H.: Large-scale spatial patterns  
464 of benthic assemblages in the SW Atlantic: the Río de la Plata, *Estuar. Coast. Shelf S.*, 61, 1-13,  
465 2004.

466 Goldberg, E. D., and Arrhenius, G.O.S.: Geochemistry of pacific pelagic sediments,  
467 *Geochim. Cosmochim. Ac.*, 13, 153-212, 1958.

468 Gómez, N. and Bauer, D. E.: Diversidad fitoplanctónica en la franja costera Sur del Río de  
469 la Plata, *Biol. Acuát.*, 19, 7-26, 2000.

470 González-Mora, B. and Sierro, F. J.: Caracterización geoquímica de las capas ricas en  
471 materia orgánica registradas durante el estadio isotópico marino 7 en el Mar de Alborán  
472 (Mediterráneo occidental), *GEOGACETA*, 43, 111-114, 2007.

473 Govin, A., Holzwarth, U., Heslop, D., Ford Keeling, L., Zabel, M., Mulitza, S., Collins, J.  
474 A., and Chiessi, C. M.: Distribution of major elements in Atlantic surface sediments (36°N–49°S):  
475 Imprint of terrigenous input and continental weathering, *Geochem. Geophys. Geosys.*, 13, 1, 1525-  
476 2027, 2012.

477 Guerrero, R., Acha, E., Framiñan, M., and Lasta, C.: Physical oceanography of the Rio de  
478 la Plata Estuary, Argentina, *Cont. Shelf. Res.*, 17, 7, 727-742, 1997.

479 Haberzettl, T., Fey, M., Lucke, A., Maidana, N., Mayr, C., Ohlendorf, C., Schabitz, F.,  
480 Schleser, G. H., Wille, M. and Zolitschka, B.: Climatically induced lake level changes during the  
481 last two millennia as reflected in sediments of Laguna Potrok Aike, southern Patagonia (Santa  
482 Cruz, Argentina), *J. Paleolimnol.*, 33, 283–302, 2005.

483 Hanebuth, T. J. J., Lantsch, H., García-Rodríguez, F. and Perez, L.: Currents controlling  
484 sedimentation: paleo-hydrodynamic variability inferred from the continental-shelf system off SE  
485 South America (Uruguay), in: *Ciencias Marino Costeras en el Umbral del Siglo XXI: Desafíos en*  
486 *Latinoamérica y el Caribe (XV COLACMAR)*, edited by: Muniz, P., Conde, D., Venturini, N. and  
487 Brugnoli, E., in press.

488 Hasle, G. R. and Syvertsen, E. E.: Marine diatoms, in: *Identifying marine phytoplankton*,  
489 edited by: Tomas, C. R., Academic Press, San Diego, California, 5-385, 1996.

490 Hassan, G.: Paleoeological significance of diatoms in argentinean estuaries, Consejo  
491 Nacional de Investigaciones Científicas y Técnicas (CONICET), Argentina, 2010.

492 Haug, G. H., Hughen, K. A., Sigman, D. M., Peterson, L. C. and Rohl, U.: Southward  
493 Migration of the Intertropical Convergence Zone through the Holocene, *Science*, 293, 1304-1307,  
494 doi: 10.1126/science.1059725, 2001.

495 Iriondo, M.: Climatic changes in the South American plains: Records of a continent-scale

496 oscillation, *Quatern. Int.*, 57-58, 93-112, 1999.

497 Jansen, J. H. F., Van der Gaast, S. J., Koster, B., and Vaars A. J.: CORTEX, a shipboard  
498 XRF-scanner for element analyses in split sediment cores, *Mar. Geol.*, 151, 1–4, 143–153,  
499 doi:10.1016/S0025 3227(98)00074-7, 1998.

500 Koffman, B. G., Kreutz, K. J., Breton, D. J., Kanel, E. J., Winski, D. A., Birkel, S. D.,  
501 Kurbatov, A. V., and Handley, M. J.: Centennial-scale variability of the Southern Hemisphere  
502 westerly wind belt in the eastern Pacific over the past two millennia, *Clim. Past*, 10, 1125–1144,  
503 doi:10.5194/cp-10-1125-2014, 2014.

504 Krastel, S., Wefer, G., Hanebuth, T. J. J., Antobreh, A. A., Freudenthal, T., Preu, B.,  
505 Schwenk, T., Strasser, M., Violante, R., and Winkelmann, D.: Sediment dynamics and geohazards  
506 off Uruguay and the de la Plata River region (northern Argentina and Uruguay), *Geo-Mar. Let.*,  
507 31, 4, 271-283, doi: 10.1007/s00367-011-0232-4, 2011.

508 Krastel, S., Wefer, G. and cruise participants: Sediment transport off Uruguay and  
509 Argentina: From the shelf to the deep sea. 19.05.2009 – 06.07.2009, Montevideo (Uruguay) –  
510 Montevideo (Uruguay), Report and preliminary results of RV METEOR Cruise M78/3, *Berichte,*  
511 *Fachbereich Geowissenschaften, Universität Bremen*, 285, 2012.

512 Lantzsich, H., Hanebuth, T. J. J., Chiessi, C. M., Schwenk, T., and Violante, R.: A high-  
513 supply sedimentary system controlled by strong hydrodynamic conditions (the continental margin  
514 off the Plata Estuary during the late Quaternary, *Quat. Res.*, 81, 2, 339-354, 2014.

515 Licursi, M., Sierra, M. V., and Gómez, N.: Diatom assemblages from a turbid coastal plain  
516 estuary: Río de la Plata (South America), *J. Marine Syst.*, 62, 33-45, 2006.

517 Löwemark, C., Chen, H., Yang, T-N., Kylander, M., Yu, E-F., Hsu, Y-W., Lee, T-Q., Song,  
518 S-R., and Jarvis, S.: Normalizing XRF scanner data: A cautionary note on the interpretation of  
519 high-resolution records from organic-rich lakes, *J. Assia Earth Sci.*, 40, 1250-1256, 2011.

520 Mahiques, M. M., Wainer, I. K. C., Burone, L., Nagai, R., Sousa, S. H. M., Lopes Figueira,  
521 R. C., da Silveira, I. C. A., Bicego, M. C., Alves, D. P. V., and Hammer, O.: A high-resolution  
522 Holocene record on the Southern Brazilian shelf: Paleoenvironmental implications, *Quatern. Int.*,  
523 206, 52-61, 2009.

524 Mahowald, N. M., Muhs, D. R., Levis, S., Rasch, P. J., Yoshioka, M., Zender, C. S., and  
525 Luo, C.: Change in atmospheric mineral aerosols in response to climate: Last glacial period,  
526 preindustrial, modern, and doubled carbon dioxide climates, *J. Geophys. Res.*, 111, D10202,  
527 doi:10.1029/2005JD006653, 2006.

528 Mann, M. E., Zhang, Z., Rutherford, S., Bradley, R. S., Hughes, M., Shindell, D., Ammann,  
529 D., Faluvegi, G., and Ni, F.: Global Signatures and Dynamical Origins of the Little Ice Age and  
530 Medieval Climate Anomaly, *Science*, 326, 1256-1259, 2009.

531 Martins, V., Dubert, J., Jouanneau, J.-M., Weber, O., Ferreira da Silva, E., Patinha, C.,  
532 Alverinho Dias, J.M., and Rocha, F.: A multiproxy approach of the Holocene evolution of shelf-  
533 slope circulation on the NW Iberian continental shelf, *Mar. Geol.*, 239, 1–18, 2007.

534 Martins, L. R., Martins, I. R., and Urien, C. M.: Aspectos sedimentares da plataforma  
535 continental na área de influencia de Rio de La Plata, *Gravel*, 1, 68-80, 2003.

536 Martins, L. R. and Urien, C. R.: Areias da plataforma e a erosão costeira, *Gravel*, 2, 4-24,  
537 2004.

538 Masello, A. and Menafrá, R.: Macrobenthic communities of the Uruguayan coastal zone and  
539 adjacent areas, in: *Río de la Plata una revisión ambiental*, edited by: Wells, P. G. and Daborn, G.  
540 R., University of Dalhousie, 140-186, 1998.

541 Massaferro, J., Perez, L., de Porras, M. E., Pérez Becoña, L., Tonello, M., and Juggins, S.:  
542 Paleocological data analysis with R, course for Latin American researchers, *Pages Magazine*,  
543 *Workshop reports*, 22, 2, 105, 2014.

544 Metzeltin, D. and García-Rodríguez, F. (Eds): *Las Diatomeas Uruguayas*, Facultad de  
545 Ciencias, Montevideo, Uruguay, 654, 2003.

546 Metzeltin, D., Lange-Bertalot, H. and García-Rodríguez, F. Diatoms of Uruguay -  
547 Taxonomy, Biogeography, Diversity, in: *Iconographia Diatomologica* (15), edited by: Lange-  
548 Bertalot, H. and Gantner Verlag, A. R. G., Koenigstein, Germany, 736, 2005.

549 Meyer, I. and Wagner, I.: The Little Ice Age in Southern South America: Proxy and model  
550 based evidence, in: *Past climate variability in South America and surrounding regions, from the*  
551 *last glacial maximum to the Holocene*, edited by: Vimeux, F., Sylvestre, F. and Khodri, M.,

552 Springer, 395-412, 2009.

553 Möller, Jr. O. O., Piola, A. R., Freitas, A. C., and Campos, E.: The effects of river discharge  
554 and seasonal winds on the shelf off southeastern South America, *Cont. Shelf Res.*, 28, 13, 1603-  
555 1624, 2008.

556 Moy, C. M., Moreno, P. I., Dunbar, R. B., Kaplan, M. R., Francois, J-P., Villalba, R., and  
557 Haberzettl, T.: Climate change in Southern South America during the last two millennia, in: *Past*  
558 *climate variability in South America and surrounding regions*, edited by: Vimeux, F., Sylvestre, F.  
559 and Khodri, M., *Developments in Paleoenvironmental Research* (14), Springer, 353-393, 2009.

560 Müller-Melchers, P.: Diatomeas procedentes de algunas muestras de turba del Uruguay.  
561 *Comunicaciones Botánicas del Museo de Historia Natural de Montevideo*, 1, 17, 1-25, 1945.

562 Müller-Melchers, P.: Sobre algunas diatomeas planctónicas de Atlántida (Uruguay),  
563 *Physis*, 20, 59, 459-466, 1953.

564 Müller-Melchers, P.: Plankton diatoms of the Southern Atlantic of Argentina and Uruguay  
565 coast. *Comunicaciones Botánicas del Museo de Historia Natural de Montevideo* 3, 38, 1-53, 1959.

566 Nagai, R. H., Ferreira, P. A. L., Mulkherjee, S., Martins, V. M., Figueira, R. C. L., Sousa,  
567 S. H. M. and Mahiques, M. M.: Hidrodinamic controls on the distribution of surface sediments  
568 from the southeast South American continental shelf between 23 S and 38 S, *Cont. Shelf. Res.*, 89,  
569 51-60, doi.org/10.1016/j.csr.2013.09.016, 2014.

570 Nogués-Paegle, J., Mechoso, C. R., Fu, R., Berbery, E. H., Chao, W. C., Chen, T.-C., Cook,  
571 K., Diaz, A. F., Enfield, D., Ferreira, R., Grimm, A. M., Kousky, V., Liebmann, B., Marengo, J.,  
572 Mo, K., Neelin, J. D., Paegle, J., Robertson, A. W., Seth, A., Vera, C. S., and Zhou, J.: Progress in  
573 Pan American CLIVAR research: Understanding the South American monsoon. *Meteorologica*,  
574 27, 3-32, 2002.

575 Perez, L., García-Rodríguez, F., and Hanebuth, T.: Paleosalinity changes in the Río de la  
576 Plata estuary and on the adjacent Uruguayan continental shelf over the past 1200 cal ka BP: an  
577 approach using diatoms as proxy, in: *Applications of paleoenvironmental techniques in estuarine*  
578 *studies*, *Developments in Paleoenvironmental Research (DPER)*, edited by: Weckström, K.,  
579 Saunders, P. and Skilbeck, G., Springer, in press.

580 Piola, A. R., Campos, E. J. D., Möller Jr., O. O., Charo, M., and Martinez C. M.:  
581 Subtropical shelf front off eastern South America, *J. Geophys. Res.*, 105, 6566–6578, 2000.

582 Piola, A. R., Moller, O. O., Guerrero, R. A. and Campos, E. J. D.: Variability of the  
583 subtropical shelf front off eastern South America: Winter 2003 and summer 2004, *Cont. Shelf*  
584 *Res.*, 28, 1639-1648, doi: 10.1016/j.csr.2008.03.013, 2008.

585 Piovano, E. L., Ariztegui, D., Cordoba, F., Cioccale, J. and Sylvestre, F.: Hydrological  
586 variability in South America below the tropic of Capricorn (Pampas and Patagonia, Argentina)  
587 during the Last 13.0 Ka, in: *Past climate variability in South America and surrounding regions,*  
588 *from the last glacial maximum to the Holocene*, edited by: Vimeux, F., Sylvestre, F. and Khodri,  
589 M., Springer, 323-352, 2009.

590 Razik, S., Chiessi, C. M, Romero, O. E. and von Dobeneck, T.: Interaction of the South  
591 American Monsoon System and the Southern Westerly Wind Belt during the last 14 kyr  
592 *Palaeogeogr. Palaeocl.*, 374, 28–40, 2013.

593 Reimer, P.J., Bard, E., Bayliss, A., Beck, J.W., Blackwell, P.G., Bronk Ramsey, C., Buck,  
594 C.E., Edwards, R.L., Friedrich, M., Grootes, P.M., Guilderson, T.P., Hafliadason, H., Hajdas, I.,  
595 Hatté, C., Heaton, T.J., Hoffmann, D.L., Hogg, A.G., Hughen, K.A., Kaiser, K.F., Kromer, B.,  
596 Manning, S.W., Niu, M., Reimer, R.W., Richards, D.A., Scott, M.E., Southon, J.R., Turney,  
597 C.S.M., and van der Plicht, J.: *IntCal13 and Marine13 radiocarbon age calibration curves 0-50,000*  
598 *yr cal BP*, *Radiocarbon*, 55, 4, 1869-1887, 2013.

599 Robertson, A. W., and Mechoso, C. R.: Interannual and interdecadal variability of the  
600 South Atlantic Convergence Zone. *Mon. Wea. Rev.*, 128, 2947-2957, 2000.

601 Romero, O. E., Lange, C. B., Fischer, G., Treppke, U. F., and Wefer, G.: Variability in  
602 export production documented by downward fluxes and species composition of marine panctonic  
603 diatoms: Observations from the tropical and ecuatorial Atlantic, in: *Use of proxies in*  
604 *paleoceanography: Examples from the South Atlantic*, edited by: Fischer, G. and Wefer, G.,  
605 *Universitat Bremen, Springer, Germany*, 365–392, 1999.

606 Salazar, A., Lizano, O. G. and Alfaro, E. J.: Composición de sedimentos en las zonas  
607 costeras de Costa Rica utilizando Fluorescencia de Rayos-X (FRX), *Rev. biol. Trop.*, 52, 2, 2004.

608 Salvatteci, R., Gutiérrez, D., Field, D. and Sifeddine, D., Ortlieb, L., Bouloubassi, I.,

609 Boussafir, M., Boucher, H and Cetin, F.: The response of the Peruvian Upwelling Ecosystem to  
610 centennial-scale global change during the last two millennia, *Clim. Past*, 10, 715–731,  
611 doi:10.5194/cp-10-715-2014, 2014.

612 Sar, E. A., Sunesen, I. and Lavigne, A. S.: *Cymatotheca*, *Tryblioptychus*, *Skeletonema* and  
613 *Cyclotella* (Thalassiosirales) from Argentinian coastal waters. Description of *Cyclotella cubiculata*  
614 sp. nov., *Vie milieu*, 60, 2, 135-156, 2010.

615 Siffedine, A., Gutiérrez, D., Ortlieb, L., Boucher, H., Velazco, F., Field, D., Vargas, G.,  
616 Boussafire, M., Salvattecí, R., Ferreira, V., García, M., Valdés, J., Caquineau, S., Mandeng Yogo,  
617 M., Cetin, F., Solis, J., Soler, P. and Baumgartner, T.: Laminated sediments from the central  
618 Peruvian continental slope: A 500 year record of upwelling system productivity, terrestrial runoff  
619 and redox conditions, *Prog. Oceanog.*, 79, 2-4, 190-197, 2008.

620 Strikis, N. M., Cruz Jr., F. W., Cheng, H., Karmann, I., Edwards, R. L., Vuille, M., Wang,  
621 X., de Paula, M. S., Novello, V. F., and Auler, A. S.: Abrupt variations in South American  
622 monsoon rainfall during the Holocene based on a speleothem record from central-eastern Brazil,  
623 *Geology*, 39, 1075–1078, 2011.

624 Urien, C. M., and Ewing, M.: Recent sediments and environment of southern Brazil,  
625 Uruguay, Buenos Aires, and Rio Negro continental shelf, in: *The Geology of Continental Margins*,  
626 edited by: Burk, C. A., and Drake, C. L., Springer, New York, 157-177, 1974.

627 Urien, C. M., Martins, L. R., and Martins, I. R.: Evolução geológica do Quaternário do  
628 litoral atlântico uruguaio, plataforma continental e regiões vizinhas, *Notas Técnicas*,  
629 CECO/URFGS, 3, 7-43, 1980.

630 Vázquez-Castro, G., Ortega-Guerrero, B., Rodríguez, A., Caballero, M., and Lozano-  
631 García, S.: Mineralogía magnética como indicador de sequía en los sedimentos lacustres de los  
632 últimos ca. 2,600 años de Santa María del Oro, occidente de México, *Rev. Mex. Cienc. Geol.*, 25,  
633 1, 21-38, 2008.

634 Vuille, M., Burns, S. J., Taylor, B. L., Cruz, F. W., Bird, B.W., Abbott, M. B., Kanner, L.  
635 C., Cheng, H., and Novello V. F.: A review of the South American monsoon history as recorded  
636 in stable isotopic proxies over the past two millennia, *Clim. Past.*, 8, 1309–1321, doi:10.5194/cp-  
637 8-1309-2012, 2012.

638 Weltje, G. J., and Tjallingii, R.: Calibration of XRF core scanners for quantitative  
 639 geochemical logging of sediment cores: Theory and application, *Earth Planet. Sci. Lett.*, 274, 3–  
 640 4, 423–438. doi:10.1016/j.epsl.2008.07.054, 2008.

641 Witkowski, A., Lange-Bertalot, H., and Metzeltin, D.: Diatom flora of marine coasts 1, in:  
 642 *Iconographia Diatomologica*, edited by: Lange-Bertalot, H., and Gantner Verlag A.R.G., 7, 925,  
 643 2000.

644 Yarincik, K., Murray, M., R. W., and Peterson, L. C: Climatically sensitive eolian and  
 645 hemipelagic deposition in the Cariaco Basin, Venezuela, over the past 578,000 years: Results from  
 646 Al/Ti and K/Al, *Paleoceanography*, 15, 2, 210–228, doi:10.1029/1999PA900048, 2000.

647 Zhou, J. and Lau, K.-M.: Does a monsoon climate exist over South America?, *J. Climate*,  
 648 11, 1020–1040, 1998.

649

650 **Table 1.** Radiocarbon dates as obtained from the Bacon modeling.

Lab # (Poz-)	Depth in core (cm)	Raw <sup>14</sup> C age (yr BP)	Bacon weighted average age (cal yr BP)	Bacon weighted average age (cal yr AD)	Sedimentation rate (cm yr <sup>-1</sup> )
35198	255	640± 30	230	1688	0.72
47935	305	775± 35	371	1494	0.68
42428	447	1000± 40	552	1293	0.78
35199	560	1090± 30	665	1167	1.00
47937	705	1220± 40	830	994	0.88
42429	964	1600± 30	1197	753	0.70

651

652

653

654

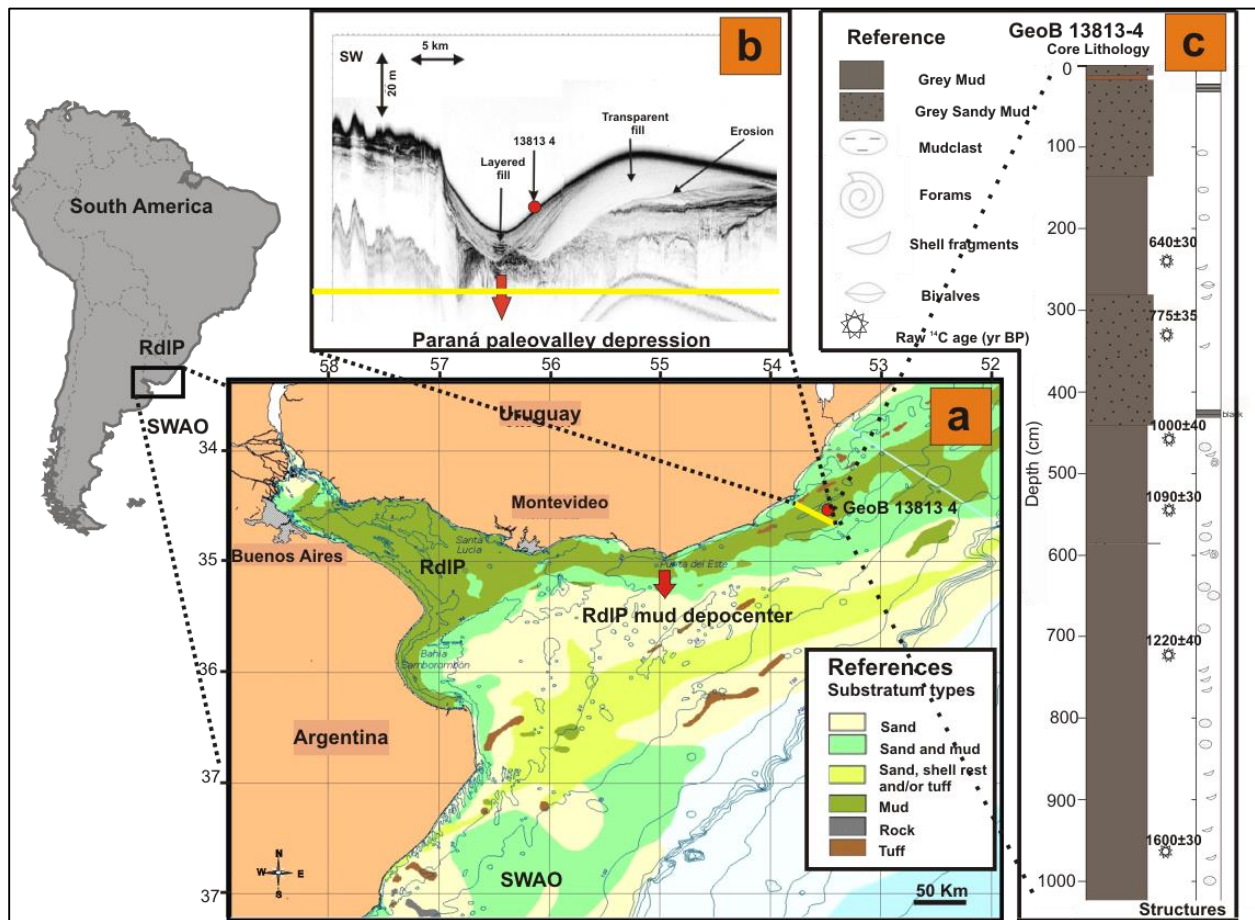


655  
656

**Table 2.** High resolution  $\delta^{18}\text{O}$  records related to SAMS changes for the MCA and the LIA.

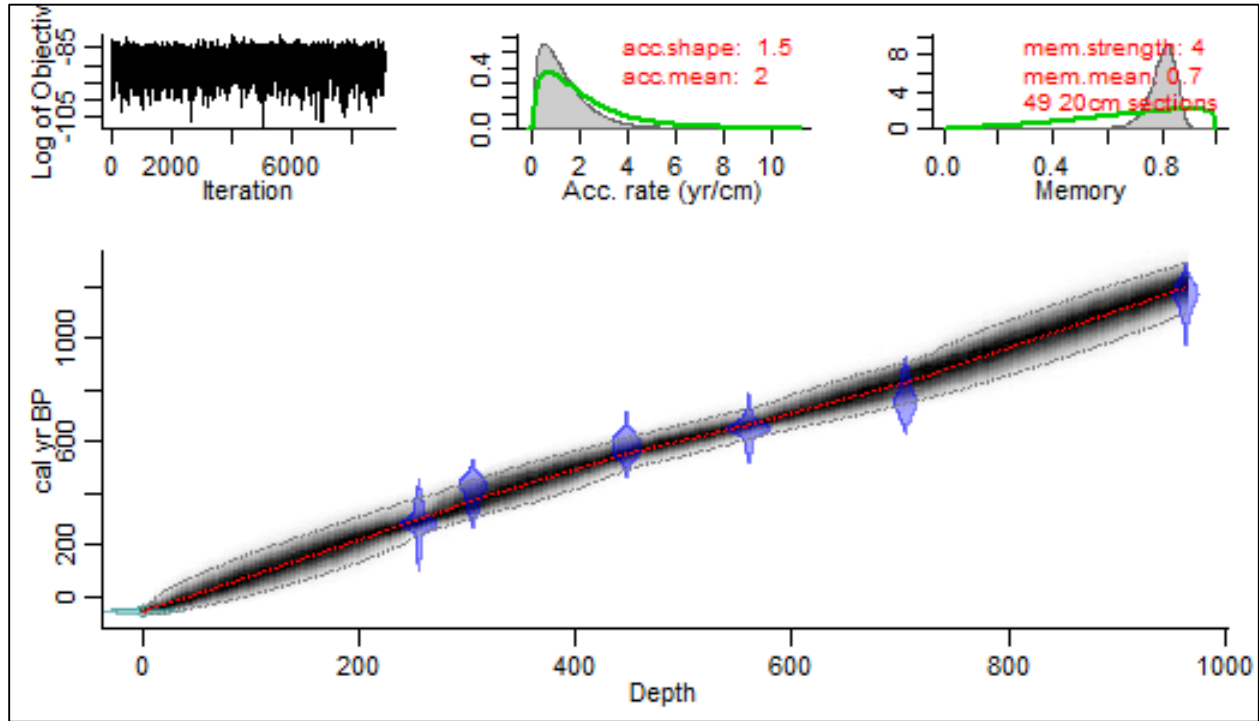
Reference	Site	Proxy	MCA	LIA	Inferred climatic context
Bird et al. (2011b)	Pumacocha Lake, Peru (Andes)	Lake sediment (calcite $\delta^{18}\text{O}$ ).	More positive $\delta^{18}\text{O}$ values (indicative of the dry season), related to a weakening of SAMS activity.	More negative $\delta^{18}\text{O}$ values (indicative of the wet season), related to a strengthening of SAMS activity.	SAMS sensitive to ITCZ and NH temperatures.
Vuille et al. (2012)	Review: Tropical Andes and SE Brazil.	$\delta^{18}\text{O}$ (Speleothem, ice and sediment cores).			SAMS modulated by changes in the North Atlantic.
Apaéstegui et al. (2014)	Palestina Cave, Peru (Andes)	Speleothem $\delta^{18}\text{O}$			SAMS modulated by AMO.

657

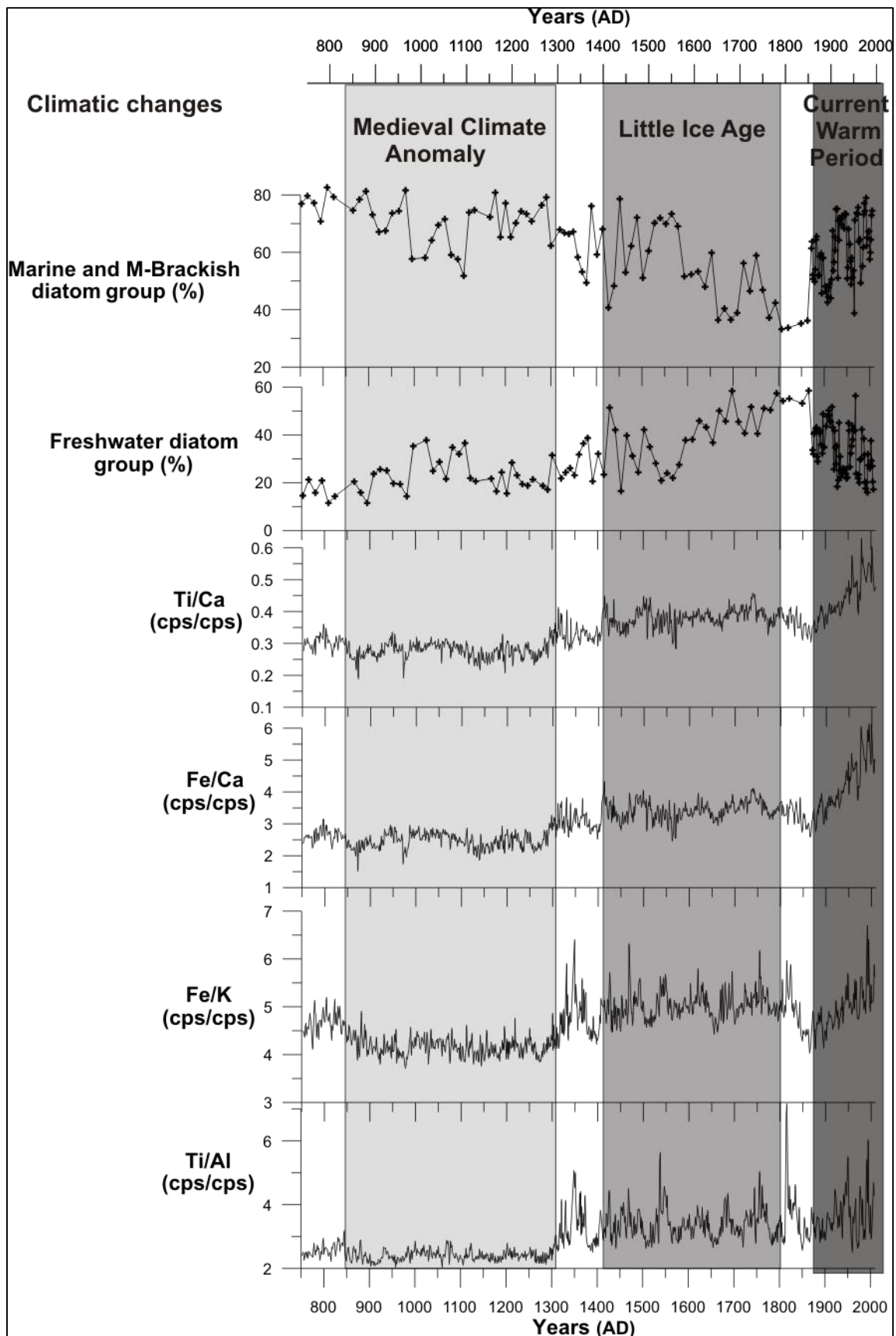


658

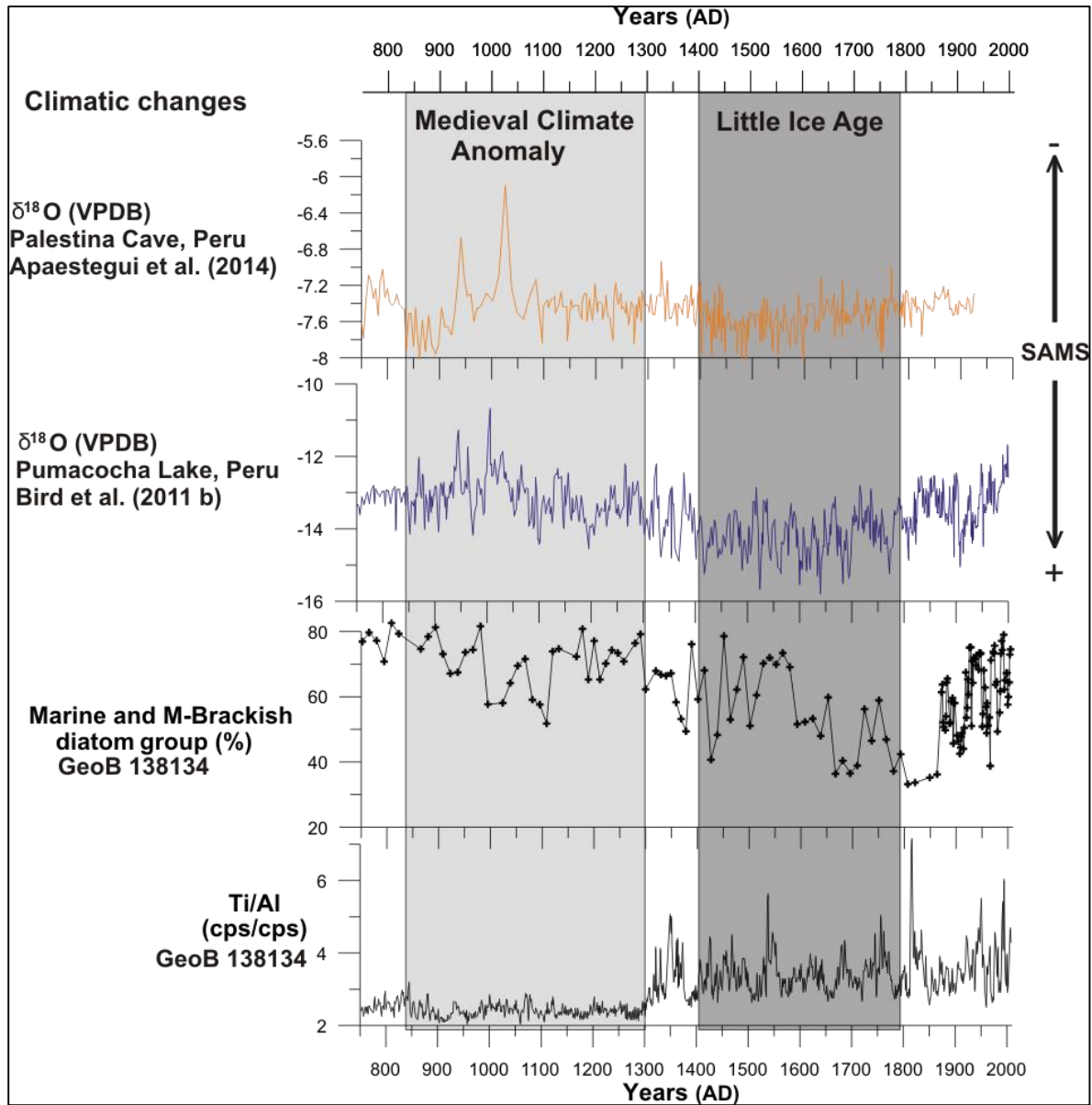
659 **Fig.1. (a)** Study area: The red circle indicates the location of Core GeoB 13813-4 retrieved from  
 660 the inner-shelf mud depocenter off the Uruguayan coast (modified from Freplata, 2004). **(b)** Rio  
 661 de la Plata (RdIP) mud depocenter (PARASOUND sub-bottom profile), which represents the RdIP  
 662 paleo-valley and its sedimentary multi-story filling succession. **(c)** GeoB 13813-4 core lithology.  
 663 (1b and 1c modified from Krastel et al., 2012 and Lantzsch et al., 2014). Stars on the right of the  
 664 sediment core indicate  $^{14}\text{C}$ -dated intervals.



665  
 666 **Fig. 2.** The age-depth model for core GeoB 13813-4 using the program Bacon. Upper panels depict  
 667 the Markov Chain Monte Carlo (MCMC) iterations (left), the prior (green curves) and posterior  
 668 (grey histograms) distributions for the sedimentation rate (middle panel) and memory (right panel).  
 669 The bottom panel shows the calibrated  $^{14}\text{C}$  dates (transparent blue), extraction year of the core (-  
 670 59 yr BP, 2009 AD, transparent blue light) and the age-depth model (grey stippled lines indicate  
 671 the 95 % confidence intervals; the red curve shows the 'best' fit based on the weighted mean age  
 672 for each depth).



674 **Fig. 3.** Centennial variation of Ti/Al, Fe/K, Ti/Ca, Fe/Ca ratios, and the freshwater and marine,  
 675 marine-brackish salinity-indicative diatom groups from the sediment core GeoB 13813-4 (from  
 676 bottom to top, respectively), during the last 1200 yr BP (750-2000 cal yr AD). The major climatic  
 677 changes during this period of time were the Medieval Climatic Anomaly and the Little Ice Age.



678

679 **Fig. 4.** Palestina Cave and Pumacocha Lake  $\delta^{18}\text{O}$  records of SAMS intensity (Apaéstegui et al.,  
 680 2014; Bird et al. 2011b), the marine, marine-brackish salinity-indicative diatom group and Ti/Al  
 681 ratios from the sediment core GeoB 13813-4 (from bottom to top, respectively) during the last  
 682 1200 yr BP (750-2000 cal yr AD). Note that the lowest  $\delta^{18}\text{O}$  values (Apaéstegui et al., 2014; Bird  
 683 et al. 2011b) are associated to higher rainfall and stronger SAMS activity, which correspond to  
 684 higher Ti/Al and lower relative abundance of marine diatoms.